Clim Dyn (2017) 49:1305–1319
DOI 10.1007/s00382-016-3381-3

Three centuries of winter temperature change on the southeastern Tibetan Plateau and its relationship with the Atlantic Multidecadal Oscillation

Shiyuan Shi[1] · Jinbao Li[2] · Jiangfeng Shi[1] · Yesi Zhao[1] · Gang Huang[3]

Received: 25 May 2016 / Accepted: 28 September 2016 / Published online: 12 October 2016

Abstract Long-term, high-resolution proxy records containing cold season temperature signals are scarce on the southeastern Tibetan Plateau (TP), limiting our understanding of regional climate and the potential driving forces. In this study, we present a nearly three centuries long reconstruction of winter (December–February) mean temperature for the central Hengduan Mountains, southeastern TP. The reconstruction is derived from a composite tree-ring width chronology of *Pinus yunnanensis* Franch from two high elevation sites (>3000 m above sea level). Our reconstruction passes all standard calibration-verification schemes and explains nearly 73 % of the variance of the original instrumental data. However, we were constrained to calibrate our full period (1718–2013) reconstruction of December–February mean temperature on the calibration period from 1959 to 1992 only, due to a decrease in temperature sensitivity of tree-ring index exhibited after 1992. Spatial correlation analysis shows that our reconstruction represents large-scale temperature variations in southwest China and the eastern TP. Our reconstructed December–February mean temperature shows a close association with the Atlantic Multidecadal Oscillation (AMO) over the past three centuries, with warm (cold) periods coinciding with the positive (negative) phases of the AMO. This persistent relationship suggests that the AMO may have been a key driver of multidecadal winter temperature variations on the southeastern TP.

Keywords Palaeoclimatology · Dendrochronology · Winter temperature · Atlantic Multidecadal Oscillation (AMO) · Southeastern Tibetan Plateau

1 Introduction

Climate has been changing dramatically since the early twentieth century (IPCC 2013). Whether recent climate change is unprecedented or still within the range of natural variability is a key scientific question (IPCC 2013; PAGES 2k Network 2013; Tingley and Huybers 2013; Wilson et al. 2016). Annually resolved, precisely dated tree-rings are crucial in this pursuit, as they provide a long-term background for assessing current climate regimes and a target for verifying climate model simulations (Collins et al. 2002; IPCC 2013).

Situated in the southeastern Tibetan Plateau (TP), southwestern China, the Hengduan Mountains are one of the earliest places where dendrochronological studies were carried out in China (Wu and Lin 1983; Wu et al. 1988; Wu and Zhao 1991). During the past decade, tree-ring studies have continued to thrive in this region (e.g., Fan et al. 2008a, b, 2009a, b, 2010; Guo et al. 2009; Fang et al. 2010; Li et al. 2011a, b, 2012, 2015; Zhao et al. 2012; Bi et al. 2015). This is due in large part to unique biological significance as

Electronic supplementary material The online version of this article (doi:10.1007/s00382-016-3381-3) contains supplementary material, which is available to authorized users.

✉ Jiangfeng Shi
shijf@nju.edu.cn

[1] Ministry of Education Key Laboratory for Coast and Island Development, School of Geographic and Oceanographic Sciences, Nanjing University, Nanjing 210023, China

[2] Department of Geography, University of Hong Kong, Pokfulam, Hong Kong, China

[3] State Key Laboratory of Numerical Modeling for Atmospheric Sciences and Geophysical Fluid Dynamics, Institute of Atmospheric Physics, Chinese Academy of Sciences, Beijing 100029, China

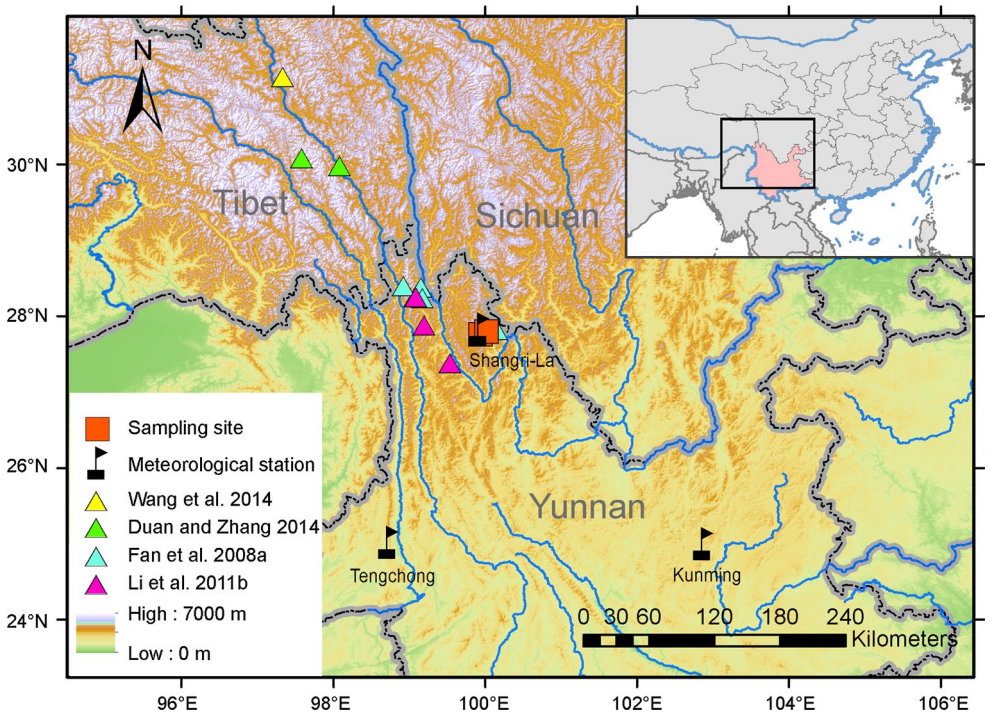

Fig. 1 Location of the sampling sites, the Shangri-La, Kunming and Tengchong meteorological stations, and the sampling sites of Fan et al. (2008a), Li et al. (2011b), Wang et al. (2014), and Duan and Zhang (2014)

a world biodiversity hotspot (Myers et al. 2000), abundant forest resources (China Forest Editing Committee 2003), and high sensitivity to global climate change (Baker and Moseley 2007; 2009b).

Previous studies revealed that radial tree growth is mainly limited by low temperature at high altitudes and water stress at low altitudes in the Hengduan Mountains (Fan et al. 2009a). Based on these response patterns, temperature reconstructions have been conducted for warm seasons at a few sites across the southeastern TP (Fan et al. 2009b, 2010; Li et al. 2011b, 2012, 2015), and for the whole year in the central Hengduan Mountains (Fan et al. 2008a). Moisture-related reconstructions have been developed in the region as well (Fan et al. 2008b; Fang et al. 2010; Li et al. 2011a, b; 2016; Bi et al. 2015). However, cold season temperature reconstructions are still scarce (Shao and Fan 1999), although significant positive responses of tree growth to winter temperature have been found in a few cases (Fan et al. 2008a, 2009a). Winter chilling damage is one of the major meteorological disasters in southwest China (Xie and Cheng 2004), and thus cold season temperature reconstructions are particularly crucial for understanding the long-term variability and the potential driving forces behind winter chilling damage. To this end, we present a new tree-ring width chronology of *Pinus yunnanensis* Franch, a tree species that has been used less frequently for dendroclimatic research, from two high altitude sites in the Hengduan Mountains, southeastern TP. As shown below, the high sensitivity of the *P. yunnanensis* Franch chronology to winter temperature allows us to develop a reliable reconstruction to perceive regional winter temperature variations during the past three centuries.

2 Data and methods

2.1 Study area and regional climate

The two sampling sites, Dabaoshi [DBS, 27°46′N, 99°47′E, 3390 m above sea level (a.s.l.)] and Luodize (LDZ, 27°48′N, 99°51′E, 3380 m a.s.l.), are located in Shangri-La, northwestern Yunnan province, southwest China (Fig. 1). This area forms the hinterland of the Hengduan Mountains on the southeastern TP. The climate of this area is characterized by alternations of the South Asian monsoon in summer and the south branch of the westerlies in winter (Duan 1997). Meteorological data used in this study are from the Shangri-La meteorological station (27°50′N, 99°42′E, 3276.7 m a.s.l.), which is the closest to the sampling sites (Fig. 1). Based on the measurements from 1958 to 2014, the annual mean temperature of Shangri-La is 6.0 °C, with the warmest monthly temperature of 13.7 °C in July and the coldest of −2.9 °C in January (Fig. 2). Annual total precipitation is 628.3 mm. The South

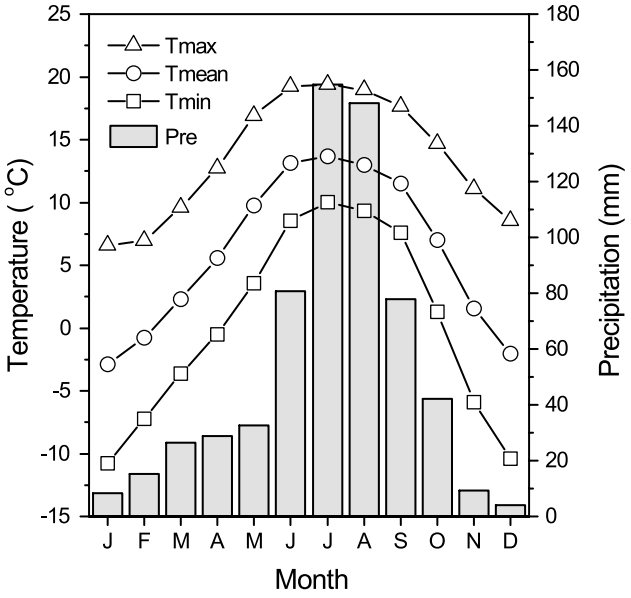

Fig. 2 Monthly mean (Tmean), maximum (Tmax), minimum (Tmin) temperatures, and monthly total precipitation (Pre) from the Shangri-La meteorological station over the period 1958–2014

Asian summer monsoon causes the warm and moist rainy season from June to October (Duan 1997), with precipitation accounting for more than 80 % of the total. The influence of the westerlies causes the dry seasons in this region from November to next May (Duan 1997). All the observed seasonal temperatures show an increasing trend, with winter temperature having the highest rising rate among all seasons and the minimum temperatures increasing faster than the maximum and mean temperature in each season (Fig. 3).

Instrumental winter temperatures from Kunming and Tengchong meteorological stations were used to validate the relationship between tree growth and winter temperature over a longer period (Fig. 1). Kunming and Tengchong meteorological stations have the earliest temperature records in Yunnan province, dating back to 1921 and 1916, respectively (Table S1). Wang (1996) interpolated the missing data and built a continuous series for each station. Winter temperature variations in Kunming and Tengchong are similar to and significantly correlated with that of Shangri-La during their common period 1959–2013 (Table S1; Fig. S1).

2.2 Tree-ring data

Following standard dendrochronological techniques (Cook and Kairiukstis 1990), we collected tree-ring samples of *P. yunnanensis* Franch from the DBS and LDZ sites in Shangri-La, southeastern TP (Fig. 1; Table 1). All samples were mounted and sanded using standard procedures (Stokes and Smiley 1968). After being visually cross-dated under

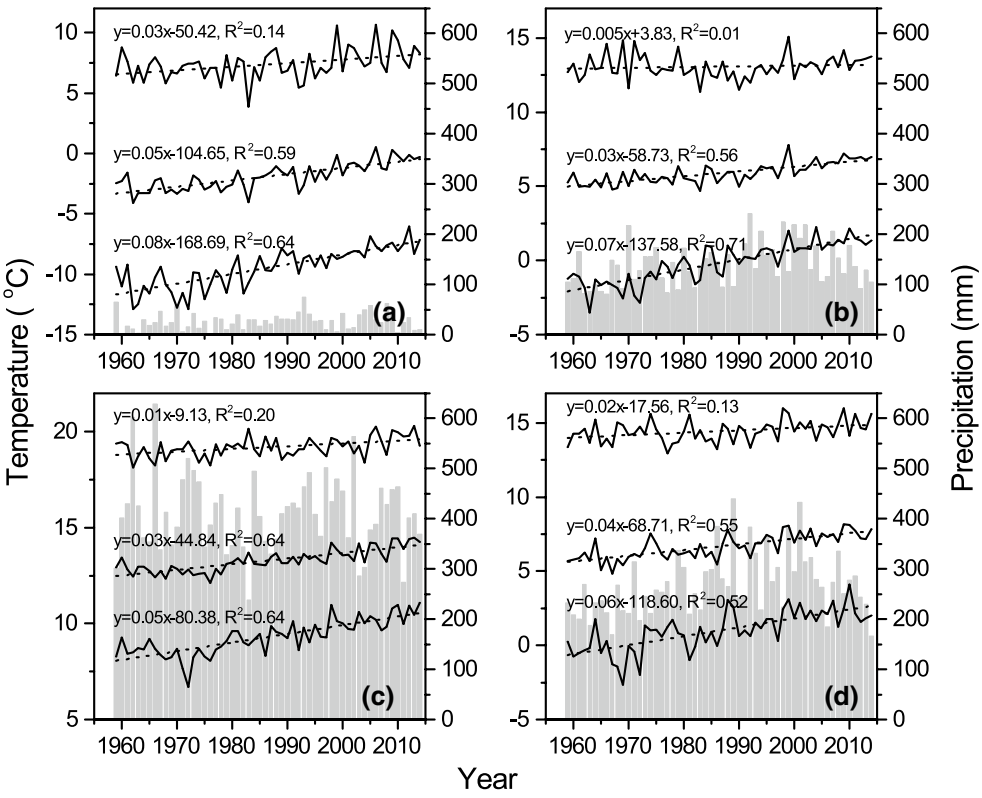

Fig. 3 Temporal changes of seasonal mean, maximum and minimum temperatures (*line*), and total precipitation (*gray bar*) in **a** December–February, **b** March–May, **c** June–August, and **d** September–November over the period 1959–2014

Table 1 Site information and tree-ring chronology statistics

Site	Location	Elev (m a.s.l.)	Number (core/tree)	Time span (A.D.)	MSL (year)	PAR (%)	MRW[a] (mm)	MS[b]	AC1[b]	EPS > 0.90 (time span/core)
DBS	27°46′N, 99°47′E	3390	61/31	1703–2013	207	0.14	0.71	0.11	0.55	1717–2013/9
LDZ	27°48′N, 99°51′E	3380	56/29	1738–2013	205	0.24	0.76	0.10	0.59	1754–2013/12
DBSLDZ	–	–	117/60	1703–2013	206	0.18	0.73	0.10	0.55	1718–2013/12

Elev elevation, *MSL* mean segment length, *PAR* percent of absent ring, *MRW* mean ring width, *MS* mean sensitivity, *AC1* first-order autocorrelation, *EPS* expressed population signal

[a] Calulated for raw ring-width values

[b] Calculated for signal-free standardized chronologies

microscope, each ring width was measured to a precision of 0.001 mm using a LINTAB 5.0 system. The quality of cross-dating was checked by the COFECHA program (Holmes 1983). Eventually, 61 cores from 31 trees of DBS and 56 cores from 29 trees of LDZ were used to develop a composite ring-width chronology.

Each raw series of measurements was detrended using the program RCSigFree (http://www.ldeo.columbia.edu/tree-ring-laboratory/resources/software). Prior to standardization, an initial power transformation was used to reduce heteroscedastic behavior commonly found in tree-rings (Cook and Peters 1997). Conservative detrending with negative exponential curves or linear regression curves of any slope was applied to detrend all series. Age-dependent spline was also applied as an additional detrending method to assess the ability of tree-rings to track recent temperature trends. Ring-width indices were calculated as residuals between actual ring-width and estimated values, and the robust biweight mean was used to assemble the chronology. We applied the "signal-free" approach to reduce potential trend distortion in tree-ring chronologies (Melvin and Briffa 2008). The Rbar weighted method was used for variance stabilization (Osborn et al. 1997). The mean inter-series correlation (Rbar) and the expressed population signal (EPS) were calculated for 51-year moving windows (Wigley et al. 1984). We used the EPS with a threshold value of 0.90 to assess the most reliable time span of each chronology.

2.3 Methods

The relationship between tree growth and climate was explored using Pearson's correlation coefficient. Kalman filter and 21-year running correlation were applied to further test whether tree growth and climate relationships were time-dependent. Kalman filter was introduced into dendroclimatology to detect time-dependent responses of trees to climate factors because it allows time-dependent regression coefficients for predictors (Visser and Molenaar 1988). The dominant climate factor of tree growth (prior winter temperature in this study) was reconstructed using a linear regression model (Cook and Kairiukstis 1990). Leave-one-out cross-validation method was employed to examine the statistical fidelity of the model due to the shortness of the overlapping period between meteorological data and the tree-ring chronology (Michaelsen 1987). The spatial representativeness of the reconstructed temperature was explored by calculating spatial correlations with the temperature data from 0.5° × 0.5° Climate Research Unit (CRU) TS3.23 grids using the KNMI climate explorer (Trouet and van Oldenborgh 2013; Harris et al. 2014). The reconstructed temperature series was also compared with other tree-ring based temperature reconstructions in nearby

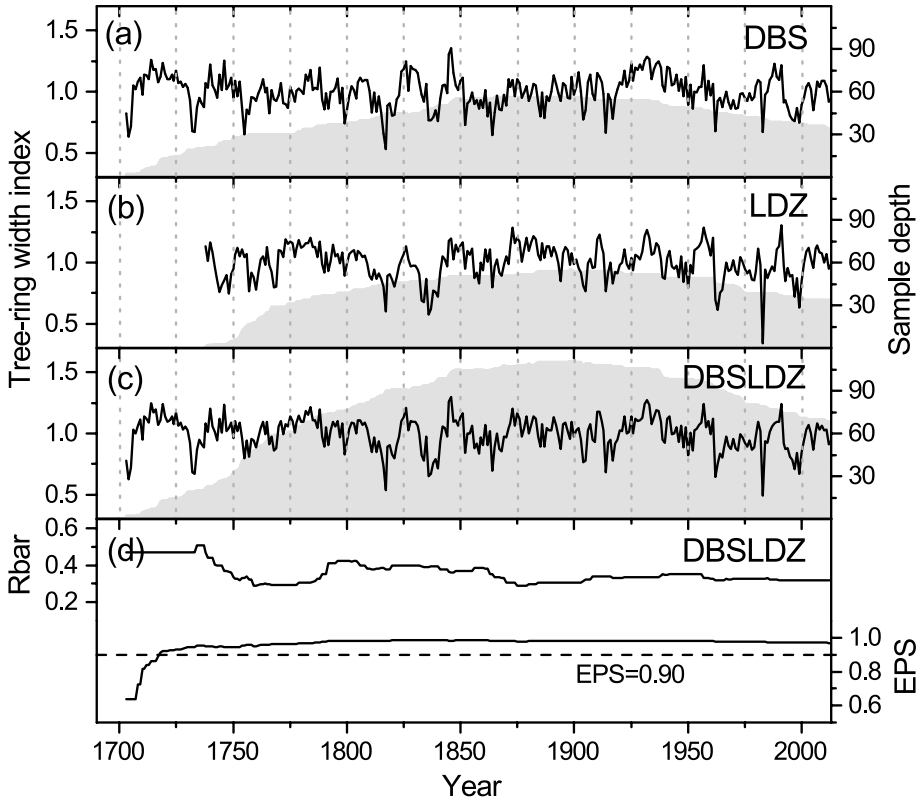

Fig. 4 **a–c** Tree-ring width chronologies of *Pinus yunnanensis* Franch from two sampling sites, the composite chronology (*line*), and their corresponding sample depth (*gray shading*), **d** the running Rbar and EPS statistics of the composite chronology. *Horizontal dashed line* denotes the 0.90 EPS cutoff value

areas to verify its reliability during the past three centuries. Finally, the reconstructed temperature series was compared with the observed and reconstructed Atlantic Multidecadal Oscillation (AMO) indices to explore its driving forces.

3 Results and discussion

3.1 Characteristics of tree-ring chronologies

A 311-year (1703–2013) and a 276-year (1738–2013) ring-width chronology was developed for DBS and LDZ, respectively (Fig. 4a, b). Comparison between the two chronologies showed that they matched well with each other and had similar statistics (Table 1). Considering the proximity of the two sites (8.3 km in direct distance) and the high correlation ($r = 0.62$, $p < 0.001$) over their common reliable period 1754–2013, we pooled all 117 samples to build a composite chronology (hereafter, DBSLDZ), with a reliable period 1718–2013 based on EPS higher than 0.90 (Fig. 4c, d). The mean sensitivity of DBSLDZ was 0.10, a typical value for conifers in humid environments (Fan et al. 2009a). The absent rings accounted for 0.18 % of the total. The inter-correlation of raw series was 0.56, indicating strong common signals in the samples.

3.2 Climate–tree growth relationships

Pearson's correlations were calculated between the composite chronology and climate factors on an 18-month window from prior May to current October for two time periods: 1959–1992 and 1993–2013 (Fig. 5). The division is identified by visual inspection and iterative correlation analyses (D'Arrigo et al. 2004a). Climate factors include monthly mean temperature (Tmean), monthly maximum temperature (Tmax), monthly minimum temperature (Tmin), and monthly total precipitation (Pre). During the earlier period 1959–1992, the correlation results showed that winter temperature was the key factor limiting radial tree growth. Tree growth responses to Tmean, Tmax and Tmin have a similar pattern, with the highest correlations in the cold season, especially from previous December to current February (Fig. 5a). This relationship indicated that winter temperature was the dominant climate factor limiting radial tree growth. The highest correlation was found between DBSLSZ and December−February mean temperature ($r = 0.85$, $p < 0.001$). Meanwhile, the influence of precipitation on radial growth was rather weak in this period, with only a marginally significant correlation found in current May. The correlation coefficients of the first difference series showed similar patterns to the raw data during this period (Fig. 5c).

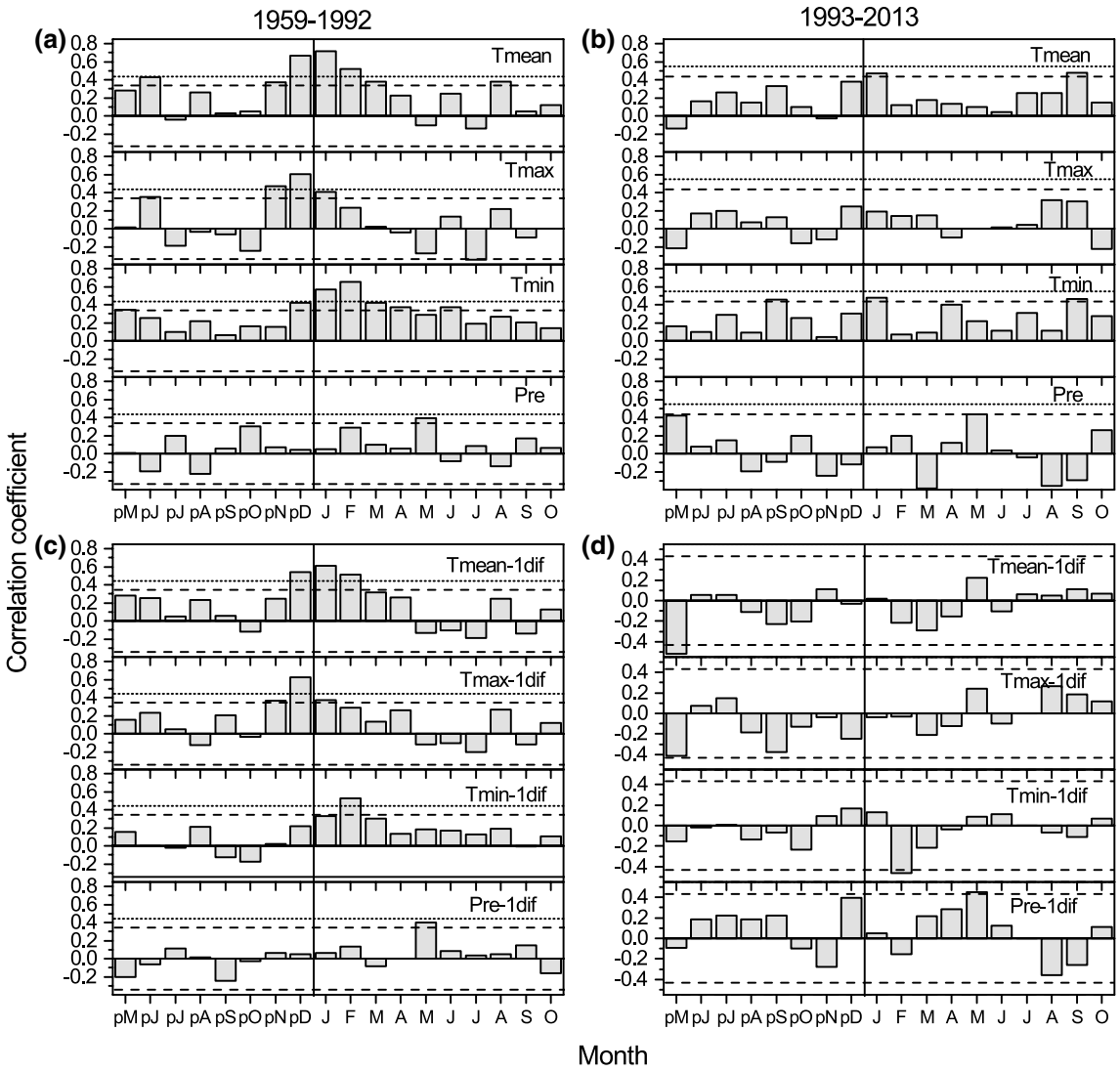

Fig. 5 Correlation coefficients between DBSLDZ chronology and monthly mean, maximum, minimum temperature and monthly total precipitation. The correlations were calculated between **a**, **b** raw series and **c**, **d** their first differences over the period **a**, **c** 1959–1992 and **b**, **d** 1993–2013. The *horizontal dashed* and *dotted lines* denote the 95 and 99 % confidence level, respectively

During the latter period 1993–2013, however, the strength of the association between DBSLDZ and cold season temperatures declined sharply, and the response of tree growth to precipitation was weak (Fig. 5b). The correlations of the first difference series dropped to be insignificant for cold season temperatures, while the correlations with precipitation remained weak (Fig. 5d). These results suggest that the marginally significant correlations with cold season temperatures during this period were largely due to trend, and prior winter temperature was no longer a controlling factor on tree growth after 1992.

We validated the relationship between tree growth and winter temperature further back in time by using two longer instrumental winter temperature series from Kunming and Tengchong meteorological stations on the southeastern TP (Wang 1996). Winter temperatures recorded at the two stations are coherent with that of Shangri-La during their common period 1959–2013 (Fig. S1; Table S1). Our ring-width chronology traced the winter temperature variations of the two stations quite well at both low- and high-frequencies before 1993, with an apparent and persistent discrepancy after 1992 (Fig. 6; Table 2). These results provide further support for the stable relationship between tree growth and winter temperature back in time and the unusual nature of their divergence after 1992.

The positive response of tree growth to winter temperature during 1959–1992 could be interpreted in terms of known physiological processes. Under low temperature, ice crystals may form in plant tissues, dehydrating cells and disrupting membranes (Körner 1998; Pallardy 2008).

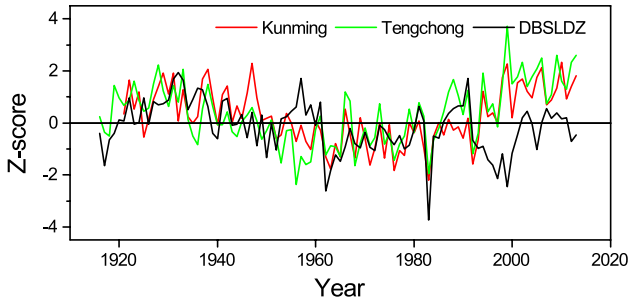

Fig. 6 Comparison of DBSLDZ and the instrumental winter temperature of **a** Kunming, and **b** Tengchong over the period 1916–2013. All series have been standardized over 1921–1992 for direct comparison

Table 2 Correlations between DBSLDZ and Kunming and Tengchong winter temperature for raw series and their first differences

Period	Kunming	Kunming (1st diff)	Tengchong	Tengchong (1st diff)
1916–1992	–	–	0.47*	0.45*
1921–1992	0.57*	0.41*	–	–
1993–2013	0.22	−0.13	0.10	−0.24

* $p < 0.01$

Frozen soil also inhibits water absorption and results in winter desiccation, damaging needles and buds and reducing trees' potential for future growth (Körner 1998; Pallardy 2008). Additionally, low temperature and deep snow cover may lead to later and slower initiation of growth in spring (Fritts 1976), shortening the growing season. In contrast, warm conditions and less physiological injuries are favorable to the synthesization and storage of carbohydrates that could be used for cambium growth of the following year (Gou et al. 2007). Similar response patterns have been reported for many tree species in high-latitude or high-altitude regions around the world (D'Arrigo et al. 1997; Pederson et al. 2004; Liang et al. 2006; Gou et al. 2007; Shi et al. 2010; Chen et al. 2012; Shi et al. 2012). In particular, this appears to be a common phenomenon for radial growth of evergreen conifers at high altitude sites in the Hengduan Mountains (Fan et al. 2008a, 2009a, b; Li et al. 2011b, 2012), and its vicinity such as the western Sichuan Plateau and southeastern Tibet (Shao and Fan 1999; Wu et al. 2006; Wang et al. 2014).

The loss in temperature sensitivity after 1992 could be a manifestation of the so-called "divergence problem" (D'Arrigo et al. 2008; Büntgen et al. 2009), which has been widely recognized in tree-rings at high northern latitudes (Jacoby and Darrigo 1995; Briffa et al. 1998; Büntgen et al. 2008), and may exist at lower latitudes as well (Bräuning and Mantwill 2004; Li et al. 2010; Chen et al. 2015). The divergence has also been noted at several sites on the eastern TP. A loss of temperature sensitivity was found in *Abies faxoniana* and *Cupressus cheniana* in Markang after an abrupt warming in 1995, and the cause was attributed to temperature-induced moisture stress (Guo et al. 2015). The growth-climate relationships of *Abies faxoniana* and *Picea purpurea* at different slope aspects in Songpan changed after the rapid warming since 1980, and soil moisture stress was likely the cause (Guo et al. 2016). Radial growth of *Abies faxoniana* showed a time-dependent relationship to climate variations in Wolong, and the combination of sunshine time decline and cloud cover increase was considered to suppress tree growth and cause recent divergence (Li et al. 2010). Moreover, the divergence phenomenon occurred at a few sites in the Hengduan Mountains as well (Fan et al. 2008a; Zhao et al. 2012), even though at a less extent and not found at all sites (Li et al. 2012, 2015).

We examined the possible cause of the divergence from several aspects in this study. First, we checked whether the common signals of tree cores decreased after 1992 by calculating a 25-year running Rbar of raw ring-width series and the prewhitened series without any detrending (Fig. S2a), and a 25-year running Rbar of ring-width series detrended by two different standardization methods (Fig. S2b). The Rbar values did not decrease in recent decades, indicating that the samples still contain strong common signals. We divided all the 117 raw ring-width series into several subsets and compared the variations of their arithmetic mean series visually to check if there is any growth divergence between different sampling sites or age-levels (Büntgen et al. 2009). As shown in Fig. S3, the ring-width variations at different subsets are similar during their common periods, suggesting that tree growth of different tree ages or sites was controlled by common environmental factors. Therefore, the cause of divergence should be a common force that influences all the samples regardless of their microenvironments or ages.

Second, we checked the homogeneity of temperature data from the Shangri-La meteorological station and its representativeness of trees' living environment. The data homogeneity was tested by comparing with the China Homogenized Historical Temperature (CHHT) dataset (1951–2004) version 1.0 released by the China Meteorological Administration (Li et al. 2009a), which provides China's most homogeneous surface air temperature series by far (Li et al. 2004). We found no bias between the two temperature datasets. We also compared the Shangri-La temperature observations with regional atmospheric background station during 2006–2012. The latter is located on top of a hill with a high vegetation coverage and low-degree influence of human activities while the former is located inside the town (Fig. S4; Yang 2015). The comparison revealed that their temperature differences could be explained by lapse rate, thus the Shangri-La records have

not been disturbed by local environmental changes, such as urbanization. In addition, we checked the winter temperature series from meteorological stations within a range of 150 km around the sampling sites and their correlations with the tree-ring chronology over the period 1959–1992 (Figs. S4, S5). All the data showed coherent correlation pattern, with that from the Shangri-La station having the highest and most stable positive correlation with tree growth (Fig. S5). Therefore, we consider that the meteorological data from the Shangri-La station represents the trees' living environment quite well.

Third, we checked whether the divergence resulted from the detrending method. We used the age-dependent spline smoothing for curve fit to build a new chronology, keeping other configurations the same as the original conservative detrending method. The curve fitting and signal-free convergence iteration differences were shown in Fig. S6. The negative exponential/linear detrending converges with 5 iterations, suggesting an overall less trend distortion than the age-dependent detrending (9 iterations). Comparison of the two chronologies with winter temperature indicated that the trend divergence still exists even if the stiffer age-dependent detrending was applied (Fig. S7b). The disagreement of year-to-year variations between tree-rings and winter temperature after 1992 cannot be resolved by any detrending method as well (Fig. S7c). These results together indicate that the divergence is not due to a failure of detrending.

Finally, we applied Kalman filter and 21-year running correlation to explore the time-dependent relationships between tree growth and climate. Table S2 shows the results of Kalman filter analysis between DBSLDZ and monthly temperatures and monthly total precipitation. Constant regression coefficient solutions were applied to most of the variables, and the changes in regression coefficients were only found in winter temperature (Fig. S8). None of the variables showed increasing tendency in regression coefficients. The results of 21-year running correlation also suggested that the stable and significant positive correlations between DBSLDZ and winter temperature weakened after 1992, without any other temperature or precipitation variables exerting a strong influence to the level as pre-1993 winter temperature for both raw series and their first differences (Fig. S9). Meanwhile, an increase in May–June precipitation sensitivity starting at about the time of the tree ring divergence from winter temperature was noted with the running correlations between the first differenced series (Fig. S9), suggesting that the early growing season moisture may have become more critical to tree growth. Nonetheless, the evidence for May–June precipitation as the new dominant controlling factor on tree growth is still weak.

In summary, the above analyses indicate that the divergence does exist between tree growth and winter temperature at our sampling sites after 1992, and that this phenomenon was not caused by common causes of divergence such as the inhomogeneity of climatic data, detrending end effect, the aging of trees, and differential response to Tmax and Tmin (D'Arrigo et al. 2008). As a result, it is hard to pinpoint the exact cause of the divergence in our study area at the current stage of our research. This is partly because the phenomenon occurred over a very short period, and partly because the phenomenon may be produced by several interwoven environmental factors.

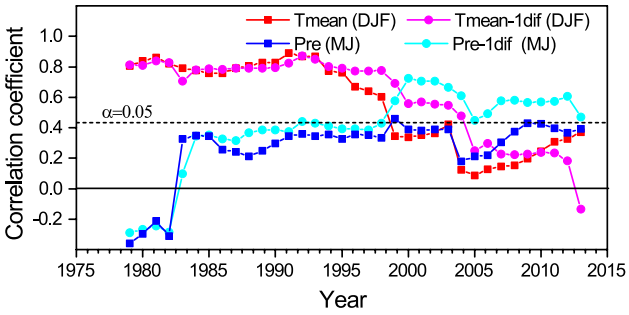

Fig. 7 The 21-year running correlations of DBSLDZ with December–February mean temperature and their first differences, and with May–June precipitation, and their first differences (every point denotes the last year of a 21-year interval). The horizontal dotted line denotes the 95 % confidence level

However, we noticed that the correlation between the first differences of DBSLDZ and May–June precipitation increased to be significantly positive at the 0.05 level at about the time when the correlation with December–February temperature dropped suddenly (Figs. 7, S9). May–June precipitation likely became the new dominant limiting factor of *P. yunnanensis* Franch growth in the study area when the role of winter temperature dropped due to rapid winter temperature increase. However, this conclusion should be accepted with caution, and further sampling of this species in the region and process-based physiological studies are needed to further test this hypothesis.

3.3 December–February mean temperature reconstruction

We reconstructed the December−February mean temperature for the period 1718–2013 using a simple linear regression model based on the calibration period 1959–1992, eliminating the recent 21 years from the calibration modeling. This method has sometimes been used when the divergence problem appeared (Jacoby et al. 2000; D'Arrigo et al. 2004b; Yonenobu and Eckstein 2006). The reconstruction accounted for 73.0 % of the actual temperature variance during 1959–1992. Leave-one-out cross-validation method was used to examine the statistical fidelity of this model due to the shortness of the calibration period

Table 3 Statistics of the leave-one-out calibration results for the common period 1959−1992

Period	R	R^2	R^2_{adj}	r	RE	RMSE	Sign test	Pmt
1959–1992	0.85*	0.73	0.72	0.83*	0.70	0.44	27/7*	3.34*

R correlation coefficient between the instrumental and reconstructed data, *r* correlation coefficient between the instrumental data and the leave-one-out-derived estimates, *RE* reduction of error, *RMSE* root mean squared error, *Pmt* product mean test

* $p < 0.01$

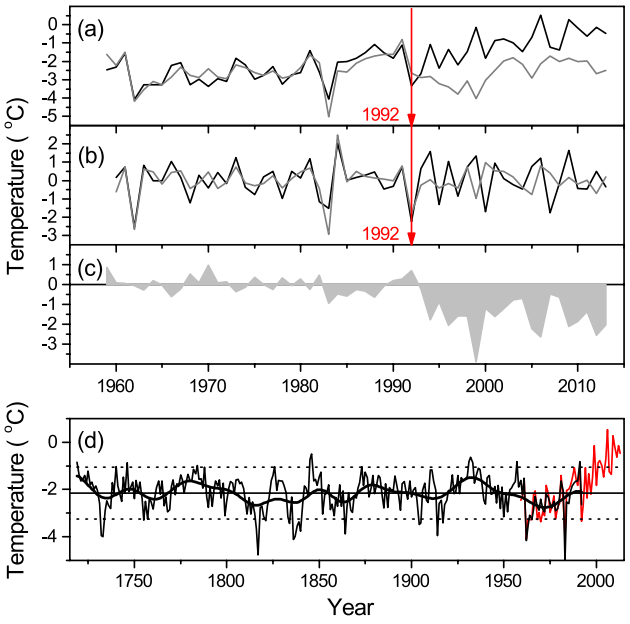

Fig. 8 December–February mean temperature reconstruction. **a** Comparison of the instrumental (*black line*) and reconstructed (*gray line*) temperature during their common period 1959–2013, **b** comparison of their first differences, **c** residuals of the reconstructed minus instrumental temperature (*gray shading*), and **d** the reconstructed temperature from 1718–1992 (*thin black line*), its 10-year Fast Fourier Transformation (FFT) smoothing (*bold black line*), the mean (*horizontal solid line*) and ±1.5 standard deviation (SD, *horizontal dotted line*) of the reconstructed temperature series over 1718–1992, and the instrumental data from 1959 to 2013 (*thin red line*)

(Michaelsen 1987). As shown in Table 3, the correlation coefficient between the actual data and the leave-one-out derived estimates was 0.83 ($p < 0.01$). The reduction of error (RE = 0.70) was highly positive, and the results of the sign-test and product mean test (Pmt) were also statistically significant, further demonstrating the validity of our regression model (Fritts 1976).

Comparison of the actual and reconstructed December−February mean temperatures indicated a high consistence until 1992, but the chronology's ability to track temperature variations decreased sharply at both high- and low-frequencies thereafter (Fig. 8a, b), and that their residuals remained negative after 1992 (Fig. 8c). Figure 8d shows the reconstructed December–February mean temperature over the past three centuries. Cold conditions prevailed in 1731–1737, 1754–1769, 1810–1843, 1856–1870, 1903–1919 and 1946–1985, while warm intervals were found in 1718–1730, 1770–1788, 1871–1890 and 1922–1945. The mean value of the reconstructed temperature series over 1718–1992 is −2.2 °C, and the standard deviation (SD) is 0.7 °C. Based on the 1718–1992 mean and SD, extremely warm winters (>mean + 1.5SD) included 1719, 1740, 1746, 1784, 1788, 1826, 1845, 1846, 1873, 1931–1933, 1957 and 1991; extremely cold winters (<mean − 1.5SD) were 1732, 1733, 1755, 1816, 1817, 1821, 1834, 1836–1840, 1864, 1904, 1905, 1914, 1917, 1962, 1963, 1965 and 1983. The winters in 1816–1817 and 1982–1983 were apparently the coldest of the past three centuries, likely due to large tropical eruptions of Mt. Tambora in 1815 and Mt. El Chichón in 1982 (Stothers 1984; Dutton and Christy 1992). In addition, 11 out of the 21 winters after 1992 were identified as extremely warm winters (1999, 2001–2003, 2005, 2006, and 2009–2013) according to observed temperature, which indicated that the most recent two decades, especially the winters after 1998, underwent an unusually persistent warming in the context of the past three centuries (Fig. 8d).

3.4 Spatial representativeness of the temperature reconstruction

Spatial correlations of the instrumental and reconstructed December–February mean temperature series and the temperature data from 0.5° × 0.5° CRU TS3.23 grids over 1959–1992 and 1993–2013 were calculated using the KNMI climate explorer. The results showed that our reconstruction captured large-scale winter temperature variability in southwest China and the eastern TP before 1993 (Fig. 9a, c). Since then, the significance level of the spatial correlations decreased, eventually reaching statistical insignificance (Fig. 9b, d).

To verify the reconstruction and to further test the temperature sensitivity of our tree-ring chronology before 1916, we compared the reconstruction with other tree-ring based temperature reconstructions close to our sampling sites (Fig. 1), including an annual mean temperature reconstruction for the period 1750–2003 using the first principal component of four spruce (*Picea brachytyla*) ring-width chronologies (Fan et al. 2008a), a reconstructed summer

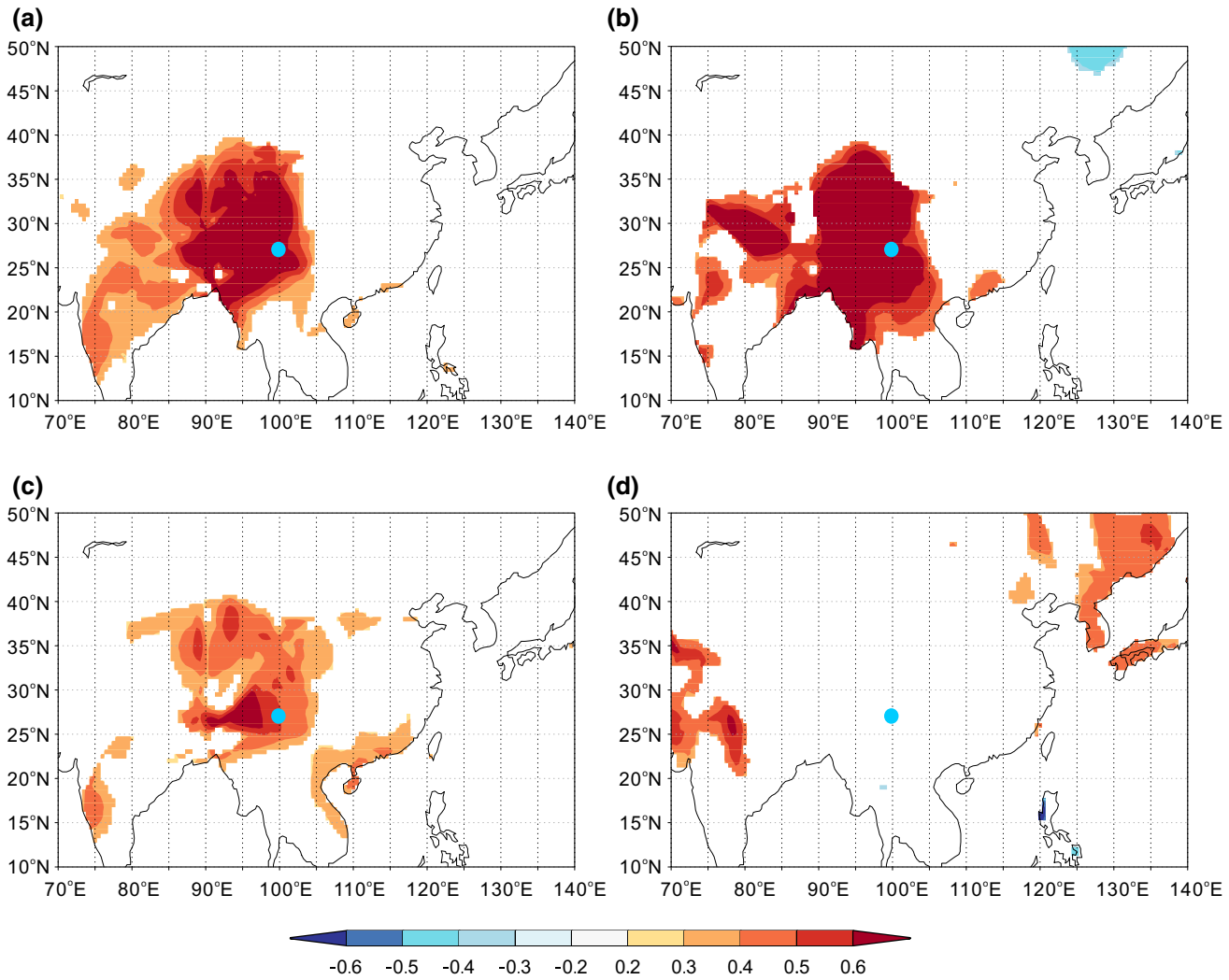

Fig. 9 Spatial correlations of **a**, **b** instrumental and **c**, **d** reconstructed December–February mean temperature series with the CRU TS3.23 land temperature over **a**, **c** 1959–1992 and **b**, **d** 1993–2013. All series have been detrended prior to spatial correlations. Insignificant correlations ($p \geq 0.1$) are masked out. The *blue dot* denotes the sampling site

(June–August) mean temperature series from 1710 to 2005 using two *Abies georgei* Orr ring-width chronologies (Li et al. 2011b), an annual mean temperature reconstruction covering the period 984–2009 using ring-width series of *Sabina tibetica* Kom. (Wang et al. 2014), and warm season (April–September) mean temperature variations since 1563 using tree-ring maximum late wood density data from *Picea likiangensis* var. *balfouriana* (Duan and Zhang 2014). It should be noted that the reconstruction of Fan et al. (2008a) was based on residual chronologies, chronologies in which low-order persistence has been removed, while the other three chronologies developed by Li et al. (2011b), Wang et al. (2014) and Duan and Zhang (2014) retained more low-frequency variance due to the use of conservative detrending methods. As shown in Fig. 10, most of the cold and warm periods matched well with each other, and the correlations were all significant at the 0.01 level. After 1992, tree-ring indices of other chronologies increased along with rising temperatures while our chronology showed an obvious trend discrepancy. These comparisons validate the temperature sensitivity of our chronology before 1916, and indicate that the post-1992 divergence was unusual over the whole reconstruction period. In addition, these reconstructions demonstrate that the period of the 2000s was the warmest over the past three centuries (Fig. S10), consistent with our result and supportive of our hypothesis that the recent extremely high temperatures induced the divergence. We also noticed that the divergence found in our research was larger than the departures between tree rings and climate records observed at the other sites in the Hengduan Mountains (Fan et al. 2008a, 2010; Duan and Zhang 2014). This phenomenon might be

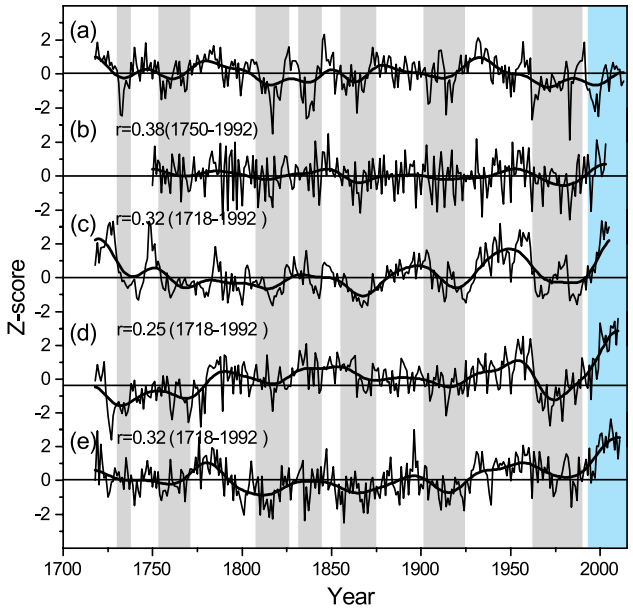

Fig. 10 Comparison of the reconstructed December–February mean temperature with four tree-ring based temperature reconstructions in the nearby regions. **a** The reconstructed December–February mean temperature from this study, **b** the annual mean temperature reconstruction in the central Hengduan Mountains (Fan et al. 2008a), **c** the June–August mean temperature reconstruction in the Baimang Snow Mountains (Li et al. 2011b), **d** the annual mean temperature reconstruction on the southeastern TP (Wang et al. 2014), and **e** the April–September mean temperature reconstruction on the southeastern TP (Duan and Zhang 2014). All series were standardized over their common period 1750–1992, and the bold lines denote the 10-year FFT smoothing. Gray bars denote their common cold period, and the blue bar denotes the divergence period 1993–2013

related to the unique physiological character of *P. yunnanensis* Franch, which was most sensitive to winter temperature that experienced most rapid increase in recent decades (Fig. 3).

3.5 Linkage with the AMO

The AMO represents the alternation of warm and cool phases in North Atlantic sea surface temperatures (SSTs) with a periodicity of roughly 70 years (Kerr 2000). It has a notable linkage with multidecadal climate variability over many regions around the globe, such as the fluctuations of global land surface temperature, precipitation in northeastern Brazil, African Sahel, Europe and North American, and Atlantic hurricanes (Knight et al. 2006; Muller et al. 2013). The coherent temperature fluctuations in North Atlantic and many parts of China have been revealed from observations, model simulations and millennium-long proxy records (Li and Bates 2007; Wang et al. 2009; Wang et al. 2013). According to the observational analysis, a positive relationship between the AMO and land surface air temperature exists in most of China, in particular its western part, and that the influence of the AMO on winter temperature is most significant on the southeastern TP (Fig. 11a; Wang et al. 2009). To investigate whether the AMO may have influenced winter temperature of the study area over a longer period, we compared our reconstruction with one instrumental and two reconstructed AMO series (Kaplan et al. 1998; Gray et al. 2004; Mann et al. 2009).

As shown in Fig. 11b, there is a visual similarity between our reconstruction and the instrumental AMO index at annual to multidecadal timescales during 1856–1992. The correlation between detrended annual series was 0.24, significant at the 0.01 level. The AMO reconstruction of Gray et al. (2004) was developed based on tree-ring records from eastern North America, Europe, Scandinavia, and the Middle East, spanning 1567–1990, while Mann et al. (2009) employed a diverse multi-proxy dataset comprising more than one thousand tree-rings, ice cores, corals, sediments, and other assorted proxy records over the past 1500 years. Our reconstruction showed coherent in-phase fluctuations with the two reconstructed AMO series on multidecadal timescales throughout the past three centuries (Fig. 11c, d). The correlations between these series (both with and without detrending) and their decadal series are all significant at the 0.01 level, as estimated using Monte Carlo simulation tests (Zhou and Zheng 1999). This finding is consistent with the study of Wang et al. (2014), however over a different season and a longer period, i.e., the past three centuries. In addition, we compared other temperature reconstructions from nearby regions (i.e., those shown in Fig. 10) with the reconstructed AMO series in the time range of our reconstruction, and found that they show consistent multidecadal fluctuations (Fig. S11). The decadal variations of the reconstructed temperature and AMO series generally correlated significantly at the 0.05 level (Table S3). The correlations between the temperature reconstruction of Fan et al. (2008a) and the AMO series were relatively low, because the former was developed from residual chronologies and contained little multidecadal fluctuations (Table S3). Dynamic analysis indicated that when the AMO is in warm phase, negative surface air pressure anomalies will form, extending from the mid-latitude North Atlantic to the middle-latitude Eurasia. The anomalous air circulation weakens the Mongolian high and cold air activity, inducing a warmer winter over East Asia (Li and Bates 2007; Wang et al. 2009; Wang et al. 2013). Together, these studies suggest that the AMO might have been an important forcing on multidecadal temperature variability on the southeastern TP.

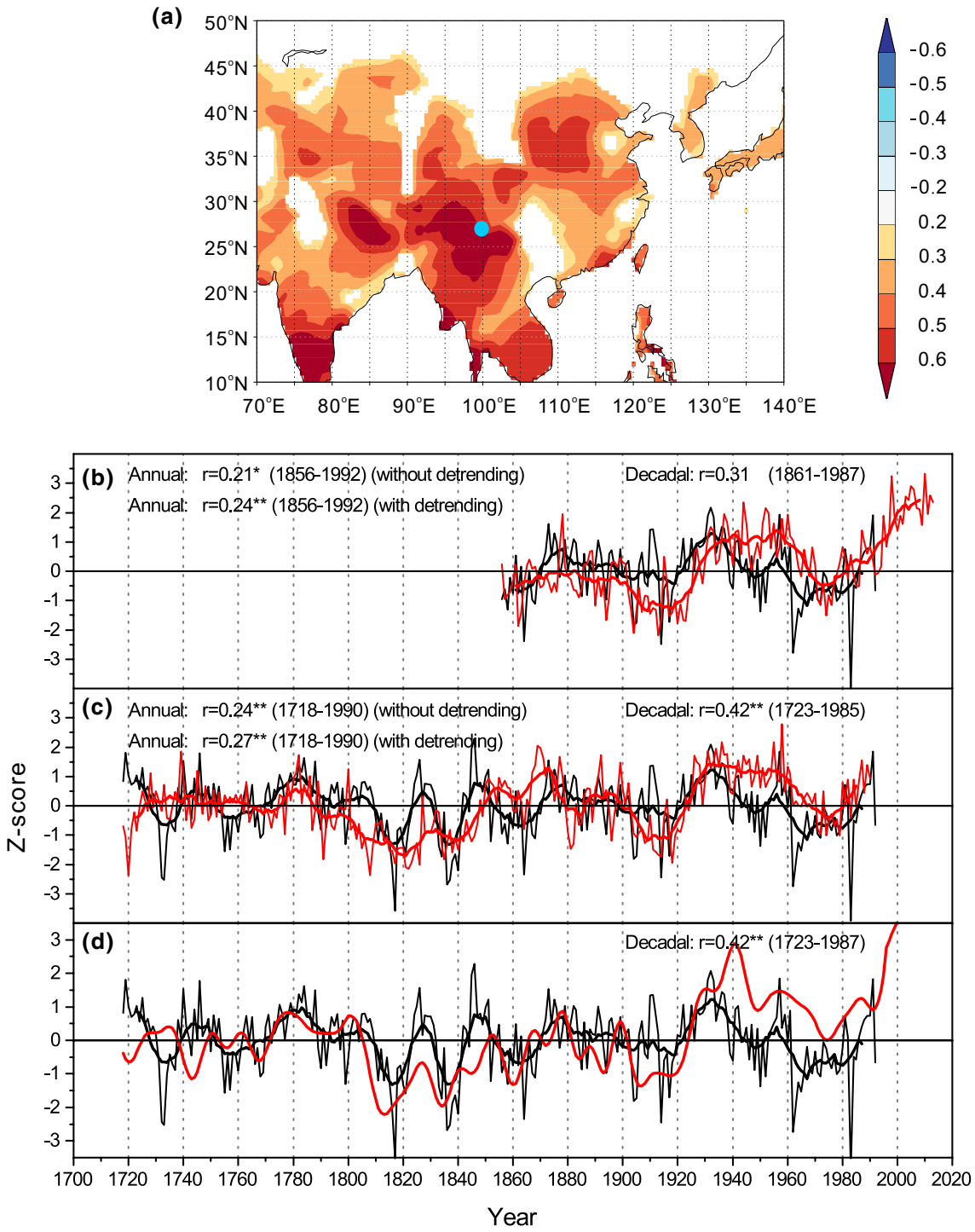

Fig. 11 The influence of the AMO on winter temperature in the study area. **a** Spatial correlation of the AMO with winter land surface temperature from the CRU TS3.23 over 1958–2013. **b**–**d** Comparison of the reconstructed December–February mean temperature with the AMO series. *Black line* in **b**–**d** denotes the reconstructed December–February mean temperature from this study (*thin line*) and its 11-year moving average (*bold line*). *Red line* **b** instrumental AMO index series from Kaplan et al. (1998) (*thin line*) and its 11-year moving average (*bold line*), **c** the reconstructed AMO index series from Gray et al. (2004) (*thin line*) and its 11-year moving average (*bold line*), and **d** the reconstructed decadal AMO index series from Mann et al. (2009) (*bold line*). The series used for comparison were standardized over their common period **b** 1856–1992, **c** 1718–1990, and **d** 1718–1992. Correlations between them are shown in each panel. *Single* (*double*) *asterisk* denotes the correlation significant at 95 % (99 %) confidence level, respectively

4 Conclusion

A 296-year robust tree-ring width chronology of *P. yunnanensis* Franch was developed from two high altitude sites in Shangri-La, southeastern TP. The chronology was used to reconstruct December−February mean temperature with an explained variance of 73.0 % over the calibration period 1959–1992. The reconstruction revealed that cold conditions prevailed in 1731–1737, 1754–1769, 1810–1843, 1856–1870, 1903–1919, and 1946–1985, while warm intervals were found in 1718–1730, 1770–1788, 1871–1890, and 1922–1945. The reconstruction represents large-scale winter temperature variations in southwest China and eastern TP. The AMO was shown to be an important forcing of winter temperature change in southwest China over the past three centuries. The period of 2000–2013 was unusually warm during the past three centuries. However, it should be accepted with caution because of the unresolved divergence problem since 1992. Further sampling of this and other tree species in the area and process-based physiological studies should be carried out in order to fully understand the divergence problem and to predict the response of regional forest ecosystem to global warming.

Acknowledgments The authors thank Yanwu Shi and Lingling Li for their help in the laboratory, Bao Yang, Jianping Duan, Zexin Fan and Zongshan Li for sharing their reconstructed temperature data, Jade d'Alpoim Guedes for improving the language, and three anonymous reviewers for their constructive comments. This research was funded by the Research Grants Council of Hong Kong (No. 27300514), the National Science Foundation of China (No. 41271210), the National Key R&D program of China (No. 2016YFA0600503), the Priority Academic Program Development of Jiangsu Higher Education Institutions, and the Jiangsu Collaborative Innovation Center for Climate Change.

References

Baker BB, Moseley RK (2007) Advancing treeline and retreating glaciers: implications for conservation in Yunnan, P.R. China. Arct Antarct Alp Res 2:200–209. doi:10.1657/1523-0430(2007)39[200:ATARGI]2.0.CO;2

Bi Y, Xu J, Gebrekirstos A, Guo L, Zhao M, Liang E, Yang X (2015) Assessing drought variability since 1650 AD from tree-rings on the Jade Dragon Snow Mountain, southwest China. Int J Climatol 35:4057–4065

Bräuning A, Mantwill B (2004) Summer temperature and summer monsoon history on the Tibetan plateau during the last 400 years recorded by tree rings. Geophys Res Lett. doi:10.1029/2004gl020793

Briffa KR, Schweingruber FH, Jones PD, Osborn TJ, Shiyatov SG, Vaganov EA (1998) Reduced sensitivity of recent tree-growth to temperature at high northern latitudes. Nature 391:678–682

Büntgen U, Frank D, Wilson R, Carrer M, Urbinati C, Esper J (2008) Testing for tree-ring divergence in the European Alps. Glob Change Biol 14:2443–2453. doi:10.1111/j.1365-2486.2008.01640.x

Büntgen U, Wilson R, Wilmking M, Niedzwiedz T, Bräuning A (2009) The 'divergence problem' in tree-ring research. TRACE Tree Rings Archaeol Climatol Ecol 7:212–219

Chen F, Yuan Y-J, Wei W-S, Yu S-L, Zhang T-W (2012) Tree ring-based winter temperature reconstruction for Changting, Fujian, subtropical region of Southeast China, since 1850: linkages to the Pacific Ocean. Theor Appl Climatol 109:141–151. doi:10.1007/s00704-011-0563-0

Chen F, Yuan Y, Wei W, Zhang T, Shang H, Yu S (2015) Divergent response of tree-ring width and maximum latewood density of *Abies faxoniana* to warming trends at the timberline of the western Qinling Mountains and northeastern Tibetan Plateau, China. Silva Fenn. doi:10.14214/sf.1155

China Forest Editing Committee (ed) (2003) China forest: coniferous forests, vol 2. China Forestry Publishing House, Beijing **(in Chinese)**

Collins M, Osborn TJ, Tett SFB, Briffa KR, Schweingruber FH (2002) A comparison of the variability of a climate model with paleotemperature estimates from a network of tree-ring densities. J Clim 15:1497–1515

Cook ER, Kairiukstis L (1990) Methods of dendrochronology: applications in the environmental sciences. Springer, New York

Cook ER, Peters K (1997) Calculating unbiased tree-ring indices for the study of climatic and environmental change. Holocene 7:361–370

D'Arrigo RD, Yamaguchi DK, Wiles GC, Jacoby GD, Osawa A, Lawrence DM (1997) A kashiwa oak (*Quercus dentata*) tree-ring width chronology from northern coastal Hokkaido, Japan. Can J For Res 27:613–617

D'Arrigo RD, Kaufmann RK, Davi N, Jacoby GC, Laskowski C, Myneni RB, Cherubini P (2004a) Thresholds for warming-induced growth decline at elevational tree line in the Yukon Territory, Canada. Glob Biogeochem Cycles 18:GB3021. doi:10.1029/2004GB002249

D'Arrigo R, Mashig E, Frank D, Jacoby G, Wilson R (2004b) Reconstructed warm season temperatures for Nome, Seward Peninsula, Alaska. Geophys Res Lett 31:L09202. doi:10.1029/2004gl019756

D'Arrigo R, Wilson R, Liepert B, Cherubini P (2008) On the 'divergence Problem' in northern forests: a review of the tree-ring evidence and possible causes. Glob Planet Change 60:289–305. doi:10.1016/j.gloplacha.2007.03.004

Duan Z (1997) Zhongdian chronicles. The Nationalities Publishing House of Yunnan, Kunming **(in Chinese)**

Duan J, Zhang QB (2014) A 449 year warm season temperature reconstruction in the southeastern Tibetan Plateau and its relation to solar activity. Palaeogeogr Palaeoclimatol Palaeoecol 119:215–240

Dutton EG, Christy JR (1992) Solar radiative forcing at selected locations and evidence for global lower tropospheric cooling following the eruptions of El Chichón and Pinatubo. Geophys Res Lett 19:2313–2316

Fan Z-X, Bräuning A, Cao K-F (2008a) Annual temperature reconstruction in the central Hengduan Mountains, China, as deduced from tree rings. Dendrochronologia 26:97–107. doi:10.1016/j.dendro.2008.01.003

Fan Z-X, Bräuning A, Cao K-F (2008b) Tree-ring based drought reconstruction in the central Hengduan Mountains region (China) since A.D. 1655. Int J Climatol 28:1879–1887. doi:10.1002/joc.1689

Fan Z-X, Bräuning A, Cao K-F, Zhu S-D (2009a) Growth–climate responses of high-elevation conifers in the central Hengduan Mountains, southwestern China. For Ecol Manag 258:306–313. doi:10.1016/j.foreco.2009.04.017

Fan Z-X, Bräuning A, Yang B, Cao K-F (2009b) Tree ring density-based summer temperature reconstruction for the central

Hengduan Mountains in southern China. Glob Planet Change 65:1–11. doi:10.1016/j.gloplacha.2008.10.001

Fan Z-X, Bräuning A, Tian Q-H, Yang B, Cao K-F (2010) Tree ring recorded May–August temperature variations since A.D. 1585 in the Gaoligong Mountains, southeastern Tibetan Plateau. Palaeogeogr Palaeoclimatol Palaeoecol 296:94–102. doi:10.1016/j.palaeo.2010.06.017

Fang K et al (2010) Reconstructed droughts for the southeastern Tibetan Plateau over the past 568 years and its linkages to the Pacific and Atlantic Ocean climate variability. Clim Dyn 35:577–585. doi:10.1007/s00382-009-0636-2

Fritts HC (1976) Tree rings and climate. Academic Press, London

Gou X, Chen F, Jacoby G, Cook E, Yang M, Peng H, Zhang Y (2007) Rapid tree growth with respect to the last 400 years in response to climate warming, northeastern Tibetan Plateau. Int J Climatol 27:1497–1503. doi:10.1002/joc.1480

Gray ST, Graumlich LJ, Betancourt JL, Pederson GT (2004) A tree-ring based reconstruction of the Atlantic Multidecadal Oscillation since 1567 A.D. Geophys Res Lett. doi:10.1029/2004gl019932

Guo G, Li Z-S, Zhang Q-B, Ma K-P, Mu C (2009) Dendroclimatological studies of *Picea likiangensis* and *Tsuga dumosa* in Lijiang, China. IAWA J 30:435–441

Guo MM, Zhang YD, Wang XC, Huang Q, Yang SX, Liu SR (2015) Effects of abrupt warming on main conifer tree rings in Markang, Sichuan, China. Acta Ecol Sin 35:7464–7474. doi:10.5846/stxb201404140715

Guo B, Zhang Y, Wang X (2016) Response of *Picea purpurea* and *Abies faxoniana* tree rings at different slope aspects to rapid warming in western Sichuan, China. Chin J Appl Ecol 27:354–364. doi:10.13287/j.1001-9332.201602.034

Harris I et al (2014) Updated high-resolution grids of monthly climatic observations—the CRU TS3. 10 Dataset. Int J Climatol 34:623–642

Holmes RL (1983) Computer-assisted quality control in tree-ring dating and measurement. Tree-Ring Bull 43:69–78

IPCC (2013) Climate change 2013: the physical science basis. Cambridge University Press, Cambridge. doi:10.1017/CBO9781107415324

Jacoby GC, Darrigo RD (1995) Tree-ring width and density evidence of climatic and potential forest change in Alaska. Glob Biogeochem Cycles 9:227–234. doi:10.1029/95gb00321

Jacoby GC, Lovelius NV, Shumilov OI, Raspopov OM, Karbainov JM, Frank DC (2000) Long-term temperature trends and tree growth in the Taymir region of northern Siberia. Quat Res 53:312–318

Kaplan A, Cane MA, Kushnir Y, Clement AC, Blumenthal MB, Rajagopalan B (1998) Analyses of global sea surface temperature 1856–1991. J Geophys Res Oceans 103:18567–18589. doi:10.1029/97jc01736

Kerr RA (2000) A North Atlantic climate pacemaker for the centuries. Science 288:1984–1986. doi:10.1126/science.288.5473.1984

Knight JR, Folland CK, Scaife AA (2006) Climate impacts of the Atlantic Multidecadal Oscillation. Geophys Res Lett. doi:10.1029/2006gl026242

Körner C (1998) A re-assessment of high elevation treeline positions and their explanation. Oecologia 115:445–459

Li S, Bates GT (2007) Influence of the Atlantic Multidecadal Oscillation on the winter climate of East China. Adv Atmos Sci 24:126–135. doi:10.1007/s00376-007-0126-6

Li Q, Liu X, Zhang H (2004) Detecting and adjusting temporal inhomogeneity in Chinese mean surface air temperature data. Adv Atmos Sci 21:260–268

Li Q, Zhang H, Liu X, Chen J, Li W, Jones P (2009a) A mainland China homogenized historical temperature dataset of 1951–2004. Bull Am Meteorol Soc 90:1062–1065. doi:10.1175/2009BAMS2736.1

Li Z et al (2009b) Changes of some monsoonal temperate glaciers in Hengduan Mountains region during 1900–2007. Acta Geogr Sin 64:1319–1330 **(in Chinese, with English abstract)**

Li Z-S, Liu G-H, Fu B-J, Zhang Q-B, Hu C-J, Luo S-Z (2010) Evaluation of temporal stability in tree growth-climate response in Wolong National Natural Reserve, western Sichuan, China. Chin J Plant Ecol 34:1045–1057. doi:10.3773/j.issn.1005-264x.2010.09.005 **(in Chinese, with English abstract)**

Li Z, Shi C, Liu Y, Zhang J, Zhang Q, Ma K (2011a) Winter drought variations based on tree-ring data in Gaoligong Mountain, northwestern Yunnan, China, A. D. 1795–2004. Pak J Bot 43:2469–2478

Li Z, Shi CM, Liu Y, Zhang J, Zhang Q, Ma K (2011b) Summer mean temperature variation from 1710–2005 inferred from tree-ring data of the Baimang Snow Mountains, northwestern Yunnan, China. Clim Res 47:207–218. doi:10.3354/cr01012

Li Z-S, Zhang Q-B, Ma K (2012) Tree-ring reconstruction of summer temperature for A.D. 1475–2003 in the central Hengduan Mountains, Northwestern Yunnan, China. Clim Change 110:455–467. doi:10.1007/s10584-011-0111-z

Li M-Y, Wang L, Fan Z-X, Shen C-C (2015) Tree-ring density inferred late summer temperature variability over the past three centuries in the Gaoligong Mountains, southeastern Tibetan Plateau. Palaeogeogr Palaeoclimatol Palaeoecol 422:57–64. doi:10.1016/j.palaeo.2015.01.003

Li J, Shi J, Zhang DD, Yang B, Fang K, Yue PH (2016) Moisture increase in response to high-altitude warming evidenced by tree-rings on the southeastern Tibetan Plateau. Clim Dyn. doi:10.1007/s00382-016-3101-z

Liang E, Shao X, Eckstein D, Huang L, Liu X (2006) Topography- and species-dependent growth responses of *Sabina przewalskii* and *Picea crassifolia* to climate on the northeast Tibetan Plateau. For Ecol Manag 236:268–277. doi:10.1016/j.foreco.2006.09.016

Mann ME et al (2009) Global signatures and dynamical origins of the Little Ice Age and Medieval Climate Anomaly. Science 326:1256–1260. doi:10.1126/science.1177303

Melvin TM, Briffa KR (2008) A "signal-free" approach to dendroclimatic standardisation. Dendrochronologia 26:71–86

Michaelsen J (1987) Cross-validation in statistical climate forecast model. J Clim Appl Meteorol 26:1589–1600. doi:10.1175/1520-0450(1987)026<1589:cviscf>2.0.co;2

Muller RA et al (2013) Decadal variations in the global atmospheric land temperatures. J Geophys Res Atmos 118:5280–5286. doi:10.1002/jgrd.50458

Myers N, Mittermeier RA, Mittermeier CG, Da Fonseca G, Kent J (2000) Biodiversity hotspots for conservation priorities. Nature 403:853–858. doi:10.1038/35002501

Osborn T, Briffa K, Jones P (1997) Adjusting variance for sample size in tree-ring chronologies and other regional mean timeseries. Dendrochronologia 15:89–99

PAGES 2K Network (2013) Continental-scale temperature variabilityduring the past two millennia. Nat Geosci 6:339–346. doi:10.1038/NGEO1797

Pallardy SG (2008) Physiology of woody plants, 3rd edn. Academic Press, Burlington

Pederson N, Cook ER, Jacoby GC, Peteet DM, Griffin KL (2004) The influence of winter temperatures on the annual radial growth of six northern range margin tree species. Dendrochronologia 22:7–29. doi:10.1016/j.dendro.2004.09.005

Shao X, Fan J (1999) Past climate on west Sichuan Plateau as reconstructed from ring-width of dragon spruce. Quat Sci 19(1):81–89 **(in Chinese, with English abstract)**

Shi JF, Cook ER, Lu HY, Li JB, Wright WE, Li SF (2010) Tree-ring based winter temperature reconstruction for the lower reaches

of the Yangtze River in southeast China. Clim Res 41:169–175. doi:10.3354/cr00851

Shi J, Li J, Cook ER, Zhang X, Lu H (2012) Growth response of *Pinus tabulaeformis* to climate along an elevation gradient in the eastern Qinling Mountains, central China. Clim Res 53:157–167. doi:10.3354/cr01098

Stokes MA, Smiley TL (1968) Introduction to tree-ring dating. University of Chicago Press, Chicago

Stothers RB (1984) The great Tambora eruption in 1815 and its aftermath. Science 224:1191–1198

Tingley MP, Huybers P (2013) Recent temperature extremes at high northern latitudes unprecedented in the past 600 years. Nature 496:201–205. doi:10.1038/nature11969

Trouet V, van Oldenborgh GJ (2013) KNMI Climate Explorer: a web-based research tool for high-resolution paleoclimatology. Tree-Ring Res 69:3–13. doi:10.3959/1536-1098-69.1.3

Visser H, Molenaar J (1988) Kalman filter analysis in dendroclimatology. Biometrics 44:929–940

Wang Y (1996) An introduction to climate change in Yunnan province. China Meteorological Press, Beijing **(in Chinese)**

Wang Y, Li S, Luo D (2009) Seasonal response of Asian Monsoonal climate to the Atlantic Multidecadal Oscillation. J Geophys Res. doi:10.1029/2008jd010929

Wang J, Yang B, Ljungqvist FC, Zhao Y (2013) The relationship between the Atlantic Multidecadal Oscillation and temperature variability in China during the last millennium. J Quat Sci 28:653–658. doi:10.1002/jqs.2658

Wang J, Yang B, Qin C, Kang S, He M, Wang Z (2014) Tree-ring inferred annual mean temperature variations on the southeastern Tibetan Plateau during the last millennium and their relationships with the Atlantic Multidecadal Oscillation. Clim Dyn 43:627–640. doi:10.1007/s00382-013-1802-0

Wigley T, Briffa KR, Jones PD (1984) On the average value of correlated time-series, with applications in dendroclimatology and hydrometeorology. J Clim Appl Meteorol 23:201–213. doi:10.1175/1520-0450(1984)023<0201:otavoc>2.0.co;2

Wilson R et al (2016) Last millennium northern hemisphere summer temperatures from tree rings: part I: the long term context. Quatern Sci Rev 134:1–18. doi:10.1016/j.quascirev.2015.12.005

Wu X, Lin Z (1983) The climatic change and tree-ring analysis in the Hsiao Zhongdian area of the Yunnan province. In: Sun H, Li W, Cheng H, Kong Z, Sun G, Zhang R, Zhang L, Zhang Y, Tong W, Su Z, Li J, Li Z, Zong G, Lin Y, Zhao E, Wu S, Gao Y, Gao D, Gao L, Tang B, Guo C, Cao W, Wen J, Pan Y, Wei J (eds) Special issue of Hengduan Mountains scientific expedition, vol 1. The Peoples Press of Yunnan, Kunming, pp 206–213 (**in Chinese, with English abstract**)

Wu X, Zhao Z (1991) Tree-ring width and climatic change in China. Quatern Sci Rev 10:545–549

Wu X, Lin Z, Sun L (1988) A preliminary study on the climatic change of the Hengduan Mountains area since 1600 A.D. Adv Atmos Sci 5:437–443. doi:10.1007/BF02656789

Wu P, Wang L, Huang L (2006) A preliminary study on the tree-ring sensitivity to climate change of five endemic conifer species in China. Geogr Res 25:43–52 **(in Chinese, with English abstract)**

Xie M-E, Cheng J-G (2004) Characteristics and formation mechanism of weather disasters in Yunnan Province. Sci Geogr Sin 24:721–726 **(in Chinese, with English abstract)**

Yang Z (2015) Shangri-La regional atmospheric background station and Shangri-La County AWS ground data analyzed. Henan Sci Technol 10:145–149 **(in Chinease, with English abstract)**

Yonenobu H, Eckstein D (2006) Reconstruction of early spring temperature for central Japan from the tree-ring widths of Hinoki cypress and its verification by other proxy records. Geophys Res Lett. doi:10.1029/2006gl026170

Zhao Z, Tan L, Kang D, Liu Q, Li J (2012) Responses of *Picea likiangensis* radial growth to climate change in the Small Zhongdian area of Yunnan Province, Southwest China. Chin J Appl Ecol 23:603–609 **(in Chinese with English abstract)**

Zhou Y, Zheng D (1999) Monte Carlo simulation test of correlation significance levels. Acta Geodaetica Cartogr Sin 28:313–318 **(in Chinese with English abstract)**